JOURNAL OF CATALYSIS 31, 243–256 (1973)

Effectiveness Factors for Peripherally Deposited Catalysts

BALJIT SINGH GAMBHIR AND ALVIN H. WEISS*

Chemical Engineering Department, Worcester Polytechnic Institute, Worcester, Massachusetts 01609

Received April 24, 1973

A flow adsorption vessel connected in series to a backmixed reactor permitted the simultaneous determination of adsorption isotherms on both catalyst and support. The multicomponent partial pressures above the support were identical to those over the catalyst in the steady state flow reactor. At high reaction rates of dichloroethylenes in H_2 over 0.5% Pt peripherally deposited on η-Al_2O_3 catalyst, there were greater amounts of reactants and lesser amounts of products adsorbed on the support than on the catalyst, even though partial pressures over each were the same. The depletion of reactants on the catalyst at high reaction rates is believed to be a combined effect of surface and gas diffusion mechanisms. The experimental method enabled an estimate to be made of the reacting species partial pressures at the interior end of the catalyst pore, behind the peripherally deposited active metal. Effectiveness factor η_{Ac} for the active metal and the maximum useful depth max L_{Ac} for metal impregnation into the pore were defined and calculated. Both η_{Ac} and max L_{Ac} were found to be dependent upon dichloroethylenes concentration and reaction rates. At fixed *trans*-$C_2H_2Cl_2$ partial pressure of 5.0 Torr, e.g., η_{Ac} decreased from 1.0 to 0.75 as the reaction rate ranged from 1.0 to 4.0 μmoles/min cc catalyst. The actual depth of metal deposition on the 1/16 in. diameter extruded pellets was 34 $\pm$ 16 μm. The maximum useful pore depth to which Pt could have been impregnated was 92 μm at 5.0 Torr *trans*-$C_2H_2Cl_2$ and a reaction rate of 4.0 μmoles/min cc catalyst.

NOMENCLATURE

C	gas concentration (moles/cc)
C_0	concentration in the bulk gas (moles/cc)
C_i	gas concentration behind the peripherally deposited active metal (moles/cc)
D	diffusion coefficient in a single pore (cm^2/sec)
D_K	Knudsen diffusion coefficient (cm^2/sec)
ϵ	effectiveness factor, i.e., ratio of measured to kinetic reaction rate
h	Thiele modulus, defined by Eq. (7)
k_{Ac}	kinetic rate constant per unit total volume of the active portion of the pellet (containing Pt)
k_s	kinetic rate constant per unit total internal surface area of the active part of the catalyst pellet
L_{Ac}	length of the active portion of pore
L_T	total length of the half pore
max L_{Ac}	useful pore depth for metal impregnation
M	molecular weight (g/mole)
n	kinetic reaction order
N_T	amount of reacting species measured on the catalyst (μmoles/g)
$\bar{r}$	average pore radius ($= 2V_g/S_g$)
S	Slope of the linear adsorption isotherm for any reacting species on support in Fig. 5,

* Correspondence.

	μmoles/g cat Torr reacting species
S_g	total N_2 BET surface area (m^2/g)
S_x	external geometrical surface area per pellet
$\bar{t}_{Ac}$	average thickness of the peripheral Pt layer
V_g	pore volume of catalyst (cc/g)
V_p	geometrical volume of a single catalyst pellet, including the pore space
η_{Ac}	effectiveness factor defined by Eq. (4)
θ	porosity of the catalyst

Introduction

Due to difficulties in measuring surface concentrations, kinetic expressions for heterogeneously catalyzed reactions are formulated on the basis of measurable gas phase concentrations surrounding the catalyst. More recently, experimental methods have been adapted for adsorption measurements during the process of surface catalysis. These include gravimetric, volumetric, gas chromatographic (*1*, *2*) and temperature programmed desorption techniques (*3*). Weiss and Gambhir (*4*, *5*) have used a flooding method (which is the basis of this present work) to measure the amounts of species present on a catalyst in a flow system at steady state. The method is useful both when a reaction is in progress and when there is no reaction taking place.

The methods cited measure the integrated amounts of adsorbate on the catalyst pellets in a reactor. A technique for measurement of the concentration gradient across one single catalyst pellet was suggested by Zeldovich (*6*) in 1939. Zeldovich's idea was experimentally demonstrated by Roiter *et al.* in 1950 (*7*). The historical development of the single pellet technique along with the recent improvements are given by Hegedus and Peterson (*8*).

Balder and Peterson (*9*, *10*) used a single pellet reactor which allowed direct measurements of the concentrations of the molecular species at the center of the symmetry plane of a pellet. They measured the hydrogenolysis reaction of cyclopropane on alumina supported platinum catalyst pellet 0.95 cm diameter $\times$ 0.6 cm long in size.

In the present study we have found that it is possible to infer the concentrations at the interior of a much smaller commercially sized catalyst pellet, in this case 1/8 $\times$ 1/16 in. diameter. The approach involves having a reacting system at steady state which is instantaneously flooded with a material that competes for the active sites of the catalyst. Reactants and products on the catalyst at the instant of flooding dissolve into the solution and provide a measure of the amounts of the species on the catalyst pellets at that instant. The model reaction chosen for study is hydrodechlorination of *cis*- and *trans*-dichloroethylenes on 0.5% platinum peripherally deposited on η-Al_2O_3 catalyst. The same reaction system was used for previous studies with the flooding method (*4*, *5*). The zero order reaction scheme is

$$\begin{array}{l} \mathrm{ClCH_2CH_2Cl} \\ +\mathrm{H_2}\uparrow \\ \mathrm{ClCH{=}CHCl} \end{array} \qquad \mathrm{ClCH_2CH_3}$$

$$\xrightarrow[-\mathrm{HCl}]{+\mathrm{H_2}} \mathrm{ClCH{=}CH_2} \xrightarrow[-\mathrm{HCl}]{+2\mathrm{H_2}} \mathrm{CH_3CH_3}$$

and the kinetics were measured by Weiss and Krieger (*11*). Pt is the active catalytic agent and alumina only serves as an inert, extended surface carrier. Isomerization of *cis*- and *trans*-dichloroethylenes is negligible in the system; and the major reaction is conversion of dichloroethylenes to vinyl chloride, which in turn, is hydrodechlorinated and rapidly hydrogenated to ethane as an observed product. Side hydrogenation reactions leading to the formation of ethyl chloride and 1,2-dichloroethane are also observed to occur.

It was reported earlier (*4*, *5*) that the measured amounts of adsorbed dichloroethylenes on the catalyst surface decreased as a function of extent of reaction rather than of partial pressure. A transition from first to zero order kinetics occurred well below monolayer coverage. Surface diffusion of physically adsorbed reactants to the dispersed Pt sites was offered as an explanation for the observed reactant depletion. The effects of reacting H_2 and product HCl on the adsorption of reacting dichloroethylenes

were not measured before. These effects will also be reported in this work, the main purpose of which will be to provide both a measure and an interpretation of the effectiveness factor concept for peripherally deposited noble metal catalysts.

Experimental Methods

1. *Catalyst and Reaction System*

The reaction system, catalyst preparation, materials, analytical methods and experimental procedures used are described elsewhere (*4*). η-Al_2O_3 support in the form of extruded pellets, 1/16 in. in diameter and of variable length, nominally 1/8 in. was supplied by Houdry Process and Chemical Co. and was impregnated with aqueous chloroplatinic acid.

Visual inspection of the cross section of broken halves of a single reduced catalyst pellet showed that Pt was deposited only on the pellet periphery. The depth of the dark black peripheral Pt layer was measured using a Reichert research metallograph and Universal camera microscope "MeF" at a magnification of 15×. Platinum deposition depth measurements were made at 10–15 different locations over the circumference of a single pellet and averaged. The metal deposition depth t_{Ae} was measured for six different pellets and averaged to give $\bar{t}_{Ae} = 34 \pm 16$ μm. Since Pt is at the pore mouths (i.e., pellet periphery) only pore length containing Pt will participate in the reaction, the pore length behind the metallic Pt will be inert.

Pt crystallite size was determined from transmission electron micrographs taken at a magnification of 348,000. Catalyst characteristics are summarized in Table 1.

TABLE 1

Catalyst pellet size:		
Av length		0.285 cm
Av diam		0.163 cm
N_2 BET surface area	S_g	190 m^2/g
H_2 Chemisorption surface area		1.34 m^2/g
Porosity	θ	0.55
Pore vol	V_g	0.38 cc/g
Pellet density	ρ_P	1.44 g/cc
True chemical density	ρ_T	3.25 g/cc
Av thickness of peripheral Pt layer	$\bar{t}_{Ae}$	34 ± 16 μm
Pt crystallite size		20 – 40 Å

2. *Adsorption Studies in the Absence of Reaction*

The reactor was also used as a vessel for flow adsorption studies. It was a U-tube fabricated from 6 mm i.d., 8 mm o.d. Pyrex glass, with a 5 mm Pyrex glass rod inserted in the effluent leg, after the catalyst bed. Adsorbent loadings of 0.3005 ± 0.0005 g were used.

Adsorption isotherms for a 50.9 mole % *cis*- and 49.1 mole % *trans*-$C_2H_2Cl_2$ mixture were measured over η-Al_2O_3 support at 32°C in the presence of HCl. Liquid dichloroethylenes feed was pumped to a vaporizer at a constant liquid hourly space velocity (LHSV) of 0.52 hr^{-1} by a Sage syringe pump equipped with a 5 cc Hamilton Teflon plunger gastight syringe. Anhydrous HCl (obtained from Matheson Co., >99% pure) was pumped by a Harvard compact infusion pump equipped with a 50 cc Hamilton Teflon plunger gastight syringe. $C_2H_2Cl_2$ and HCl feed streams were fed from their pump syringes to the adsorption system through Teflon capillaries. HCl gas flow rates ranged from 0.0092 to 0.193 SCCM, giving HCl partial pressures between 0.094 and 2.01 Torr. Helium flow rate was fixed at 70 SCCM. When adsorption steady state (as measured by effluent analysis) was reached, the reactor was flooded with 3.5 cc of CCl_4. Organic species in the CCl_4 were measured gas chromatographically. The CCl_4 solution contained no measurable HCl. The adsorbent pellets were then transferred to a bottle containing 25 cc of distilled water and the total mixture of adsorbent and water was titrated with 0.025 *N* NaOH to a methyl red end point. The titrated slurry was then refluxed, titrated and refluxed again till no further acidity was imparted to the solution upon heating.

In addition to the method described above, flow adsorption–desorption experi-

ments for gas mixtures of varying partial pressures of dichloroethylenes and HCl in 70 SCCM He were also made on both catalyst and support. Activation was in flowing He + H_2 at 190°C for 2.5 hr. Adsorbent temperature was fixed at 32°C. Effluent gas at the reactor exit passed through a train of two 250 cc Erlenmeyer flasks containing about 75 cc of distilled water each to absorb HCl. More than 99% HCl absorption took place in the first flask. At steady state, when both HCl and $C_2H_2Cl_2$ partial pressures in the effluent stream equalled those in the feed, the adsorbate feed stream was abruptly switched to pure He at 70 SCCM over the adsorbent. The temperature of the adsorbent was kept constant at 32°C. The desorbate stream was absorbed in water and monitored till the HCl concentration in the effluent stream reduced to zero. Total HCl purged from the catalyst by the flowing helium corresponds to the cumulative amount of HCl which was *physically* adsorbed. When the physically adsorbed HCl was purged off, the adsorbent was flooded with water and the water solution titrated for the HCl remaining on the adsorbent. This provided a measure of the HCl quantity *chemisorbed*.

Experiments were also made using two identical U-tube vessels in series. The arrangement is shown in Fig. 1, and, as with the preceding work, each vessel was fabricated from 6 mm o.d., 8 mm o.d. Pyrex glass, with a 5 mm Pyrex glass rod inserted in the effluent side. Product gases from the first vessel (the reactor) containing Pt on Al_2O_3 catalyst were fed to the second vessel containing only the Al_2O_3 support (without Pt). This permitted adsorption to proceed at partial pressures identical to those in the reactor outlet. Both the catalyst and support (loadings of 0.3005 ± 0.0005 g each) were activated *in situ* in flowing He + H_2 for 2.5 hr at 190°C. At steady state, the gas feed stream to the vessels was bypassed and simultaneously 3.5 cc of liquid CCl_4 were injected into each vessel. Appropriate blank corrections were applied by subtracting the amounts of *cis*- and *trans*-$C_2H_2Cl_2$ present in the empty vessel from the adsorption quantities measured when adsorbent was used.

Results

Adsorption isotherms obtained in the flow mode in the absence of HCl for dichloroethylenes at 32°C, LHSV = 0.52 hr^{-1} over η-Al_2O_3 are plotted in Fig. 2. Both He and He + H_2 (610 Torr) were used as diluent gases. Figure 2 shows that H_2 has a minor depletive effect on adsorption of both *cis*- and *trans*-$C_2H_2Cl_2$.

Figure 3 shows the effect of HCl on the adsorption of *cis*- and *trans*-$C_2H_2Cl_2$ on sup-

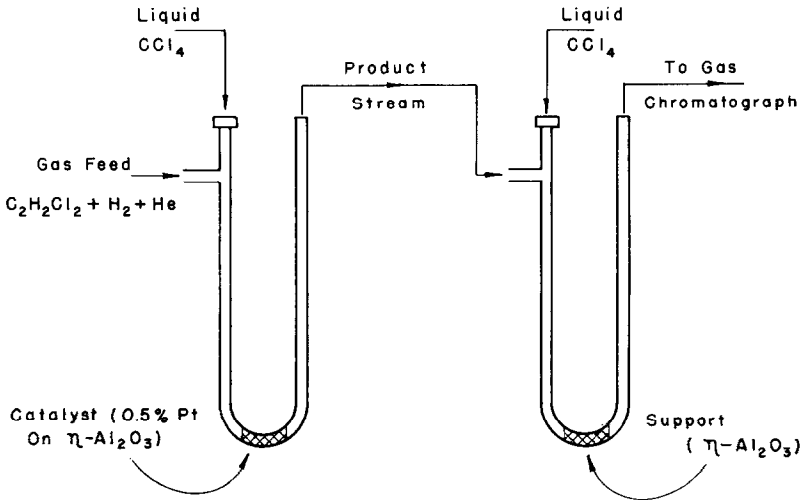

FIG. 1. Series experiments. Flooding both vessels at steady state allows measurement of adsorption on both catalyst and support at conditions identical to those over the catalyst.

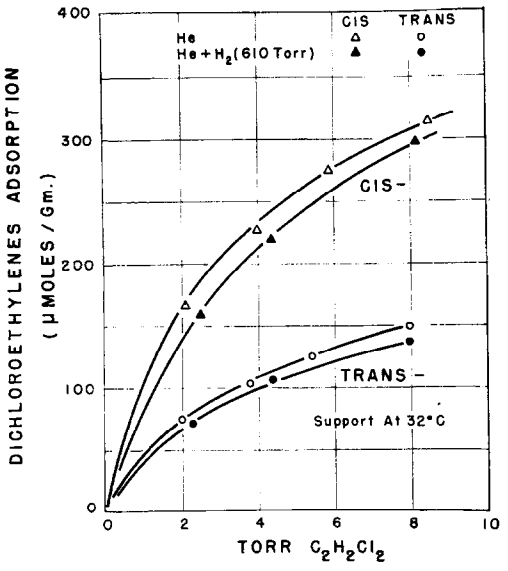

FIG. 2. Hydrogen has a minor depletive effect on adsorption of both *cis*- and *trans*-$C_2H_2Cl_2$.

port in He at 32°C, LHSV = 0.52 hr^{-1} and fixed dichloroethylenes partial pressure of 10.6 Torr. The amounts of adsorbed *cis*- and *trans*-$C_2H_2Cl_2$ both decrease as a function of pHCl up to about 0.5 Torr. Above this HCl partial pressure, the amounts of adsorbed $C_2H_2Cl_2$ are unaffected by competitively adsorbed HCl.

Adsorption of dichloroethylenes (10.6 Torr) in HCl (0.19 Torr) at 32°C was measured at nonreacting conditions both over support by using He + H_2 (580 Torr) as a diluent gas instead of He alone and over catalyst instead of support as the adsorbent with He as the diluent gas. These data are also plotted in Fig. 3. Almost identical $C_2H_2Cl_2$ adsorptions at nonreacting conditions were obtained on catalyst (in He) and on support (in He or He + H_2). The presence of either H_2 in the gas or Pt on the catalyst does not influence the adsorption of dichloroethylenes at a fixed HCl partial pressure.

Figure 3 also shows adsorption data obtained under reacting conditions. $C_2H_2Cl_2$ LHSV was varied from 0.25 to 3.85 hr^{-1} at fixed partial pressures of 48.5 Torr H_2 and 10.6 Torr $C_2H_2Cl_2$ (feed) at 32°C over a fractional conversion range of 0.006–0.20 (*4*). HCl partial pressure was calculated

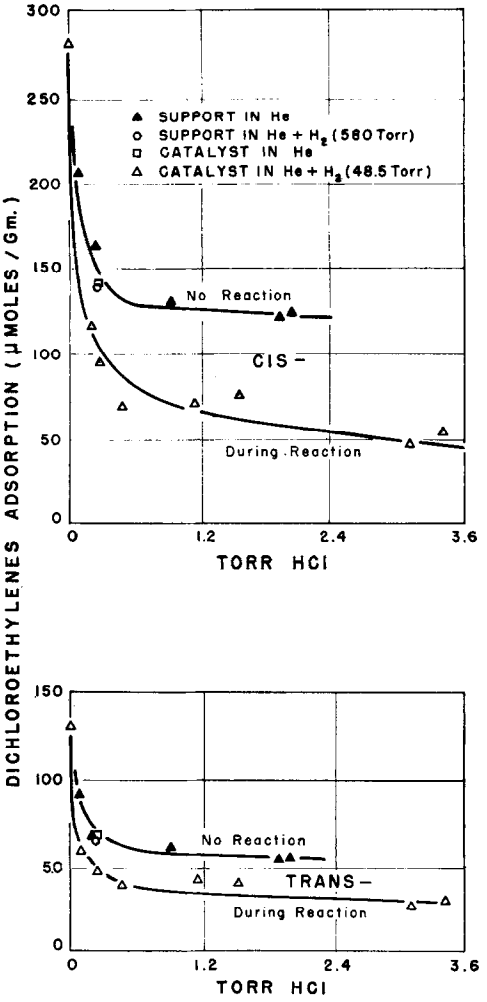

FIG. 3. $C_2H_2Cl_2$ adsorption at 10.6 Torr, 32°C. The depletion of $C_2H_2Cl_2$ on the catalyst during reaction is greater than that accounted for by the presence of HCl alone.

from the product gas analysis and the known stoichiometry of the reaction.

Figure 3 shows that at fixed HCl and dichloroethylenes partial pressures there is less dichloroethylenes adsorbed on catalyst under reaction conditions than on support or catalyst in the absence of reaction. The depletion of $C_2H_2Cl_2$ on the catalyst under reacting conditions takes place to a greater extent than that accounted for by the competitive adsorption alone.

Figure 4 shows that HCl is adsorbed in large relative quantities compared with adsorption of both *cis*- and *trans*-$C_2H_2Cl_2$.

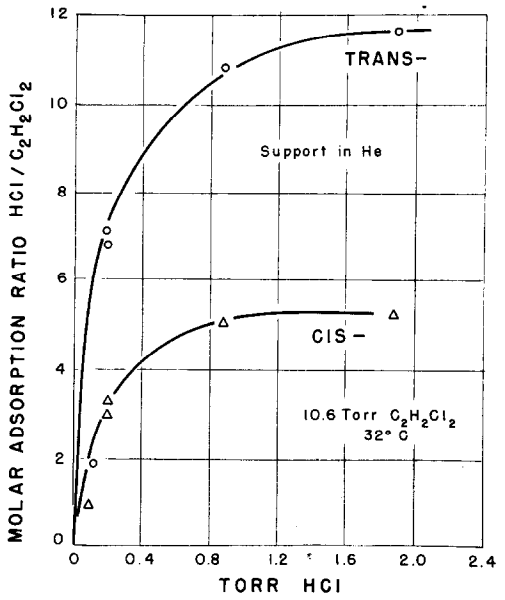

FIG. 4. HCl is adsorbed in large relative quantities compared with adsorption of both *cis-* and *trans-* $C_2H_2Cl_2$.

Table 2 summarizes the results of the desorption dynamics studies for support and catalyst brought to adsorption steady state. More than 90% of the HCl adsorption by the support occurred in the first hour. Seventy percent of the physically adsorbed HCl desorbed in 3 hr. The support did not have any measurable acidity. The catalyst had an acidity of 12.6 μmoles/g probably due to HCl left on the surface during reduction of H_2PtCl_6 to Pt. The majority of HCl is chemisorbed.

Scanning electron micrographs with a Cambridge Stereo Scan Mark 2A microscope were obtained for fresh (reduced) and for aged catalyst pellets at magnifications of 525 and 2100. Both exterior surfaces and the fractured cross sections of the pellets were scanned. Surface transmission electron micrographs were also obtained for both fresh and aged catalyst at magnifications of 288,000 and 348,000. The catalyst was aged at $pC_2H_2Cl_2$ = 33.0 Torr, pH_2 = 570 Torr and a reaction temperature of 32°C for 9 hr (these reaction conditions approached the severest for the entire study). Scanning and transmission electron microscopic analyses revealed no noticeable changes in the morphology of either fresh or aged catalyst samples (*12*). Temperature increases on the catalyst surface and within a catalyst pellet resulting from the exothermic hydrodechlorination reactions were calculated by the methods of Anderson (*13*), or Mears (*14*) and of Bercovich and Jaime (*15*), as well as measured experimentally. The experimental measurement of temperature involved inserting a 0.0303 cm diameter thermocouple into a fine hole (0.0440 cm) drilled in the axis of one of the 1/16 in. diameter pellets in the reactor. Heat conduction along the thermocouple wire could result in a measured temperature rise lower than the true value (for reaction conditions approaching the severest for the entire study). Calculated and experimentally measured temperature differences (*12*) amounted to only 3.5 and 1.3°C maximum, respectively, which are insufficient to significantly affect either the rates or the adsorbed quantities.

TABLE 2
MOST OF HCl IS CHEMISORBED[a]

	μmoles/g on	
	Support	Catalyst
Reacted with adsorbent	160	122
Physically adsorbed	180	216
Chemisorbed	484	462
Unaccounted	52	
Total by material balance	876	800

[a] 32°C, 1.84 Torr HCl, 10.4 Torr $C_2H_2Cl_2$.

Series experiments were made using approximately an equimolar *cis-* and *trans-* $C_2H_2Cl_2$ feed mixture at 32°C reaction temperature, 0.52 LHSV and varying H_2 and $C_2H_2Cl_2$ concentrations. Since the first vessel (the reactor containing the catalyst) behaves as a backmixed reactor, both catalyst in the reactor and support in the vessel following the reactor are subjected to the same gaseous product concentrations. Since the adsorbed quantity of any species on catalyst is only a function of its gas phase concentration and remains unaffected by reaction, its amount on both the catalyst and support should be identical, if no other phenomenon affects adsorption–desorption.

TABLE 3
SERIES EXPERIMENTS AT 32°C, 0.52 LHSV

Reactor effluent (Torr)		Total conv.	Reaction rate (μmoles/	Quantities of *trans* adsorbed (μmoles/g)	
H_2	*trans*	%	min cc cat)	On catalyst	On support
47.2	5.11	5.75	6.7	53.8	53.0
53.8	4.92	3.28	3.8	49.9	53.2
610.9	2.63	39.2	45.8	8.4	27.4
582.0	0.96	37.9	43.3	0.42	11.7

Results obtained for *trans*-$C_2H_2Cl_2$ are summarized in Table 3. Degree of dispersion calculations indicate that in all of the experiments listed, the reactor was effectively back-mixed, as was the case in earlier work (*4*, *5*, *12*). It can be seen that at low reaction rates (3.8 and 6.7 μmoles/min cc catalyst) identical amounts are adsorbed on both catalyst and support, implying that the entire internal pore surface of the catalyst is available for adsorption at the bulk gas concentration. At high reaction rates (≈45 μmoles/min cc catalyst) the amounts adsorbed on peripherally deposited catalyst range from 4 to 30% of that measured on support. The depletion is more pronounced with decreasing $C_2H_2Cl_2$ gas concentration at identical observed reaction rates. Similar results were obtained for *cis*-$C_2H_2Cl_2$.

The measured amounts of the different species on catalyst and support in the series experiments are plotted against effluent gas phase concentrations (measured at the outlet of the second vessel) in Fig. 5 (for reacting species) and in Fig. 6 (for product species). All the data are for pHCl > 0.5 Torr, where HCl was found to have a constant effect on dichloroethylenes adsorption. Figures 5 and 6 show at partial pressures that correspond to low reaction rates, that adsorbed quantities of both reactants and products measured on the catalyst are identical to those measured on support. At high reaction rates, reactants deplete and products accumulate on catalyst relative to their respective amounts on support. This type of behavior is characteristic of pore diffusion phenomenon. Thus, at high reaction rates, both surface diffusion and pore diffusion effects combine to cause the total observed depletion of reacting species on the catalyst.

INTERPRETATION OF RESULTS

An idealized pellet pore structure can be regarded as an assemblage of cylindrical pores of identical average radius and average length (*16–18*). An average catalyst pore with various dimensions is shown in Fig. 7. L_{Ac} is the active length, i.e., the depth of the peripherally deposited metal. Calculated value of the average radius $\bar{r}$ is 40.4 Å, which is in the micropore regime. Although dichloroethylenes reaction to ethane is accompanied by a mole number change, such a large excess of H_2 and He was used in this study that the effect of volume change is negligible. Vectors suggesting gas-phase diffusion, adsorption–desorption, and surface diffusion are also drawn on Fig. 7. C_0 represents bulk gas reactant concentration, C_i that in the pore behind the active metal.

If gas diffusion is the only means of transport into the pore, the steady state conservation equation incorporating a power law rate expression for reacting dichloroethylenes (*trans*- or *cis*-) in a single pore is (*17*):

$$D\frac{d^2C}{dx^2} = \frac{2k_sC^n}{\bar{r}}. \qquad (1)$$

There is no reaction and hence no flux past the active length of the pore i.e., at $x = L_{Ac}$. The concentration gradient must be zero at this point. The boundary conditions for the conservation Eq. (1) are

$$\begin{aligned} x &= 0 \qquad C = C_0 \\ x &\geq L_{Ac} \qquad C = C_i \qquad \frac{dC}{dx} = 0. \end{aligned} \qquad (2)$$

Gas concentration gradients for a peripherally deposited pore are shown in Fig. 8. For simplicity, a linear concentration profile in the gas phase is assumed over the active length of the pore L_{Ac}.

The conservation Eq. (1) and its boundary conditions for the single pore are those for a single pellet reactor, such as used by Balder and Peterson (*9*). The total pellet length

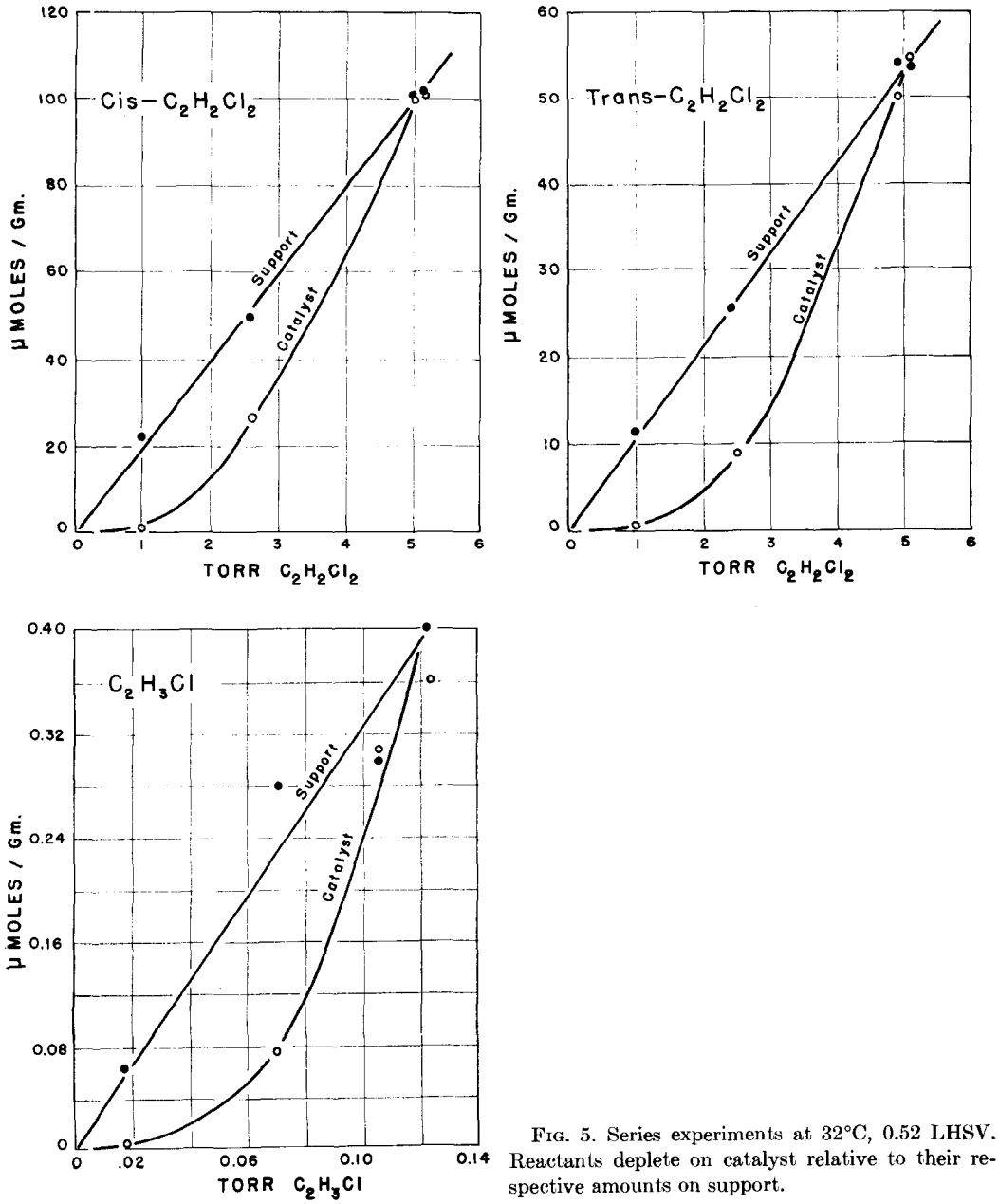

FIG. 5. Series experiments at 32°C, 0.52 LHSV. Reactants deplete on catalyst relative to their respective amounts on support.

and center plane chamber in a single pellet reactor correspond, respectively, to the active length L_{Ac} and inert pore length (beyond L_{Ac}) of a peripherally deposited catalyst pore. The concentration C_i of the reacting species in the center plane chamber is analogous to concentration C_i in the inert length of the pore in the example on Fig. 8. Calculated concentration gradients for various reaction orders can be used as a more rigorous solution to the system than the simplified assumption of linear concentration gradient across the active metal that we use.

The quantities of species measured on the catalyst in the series experiments correspond to the integrated amount under the concentration profile that is shown in Fig. 8 for a

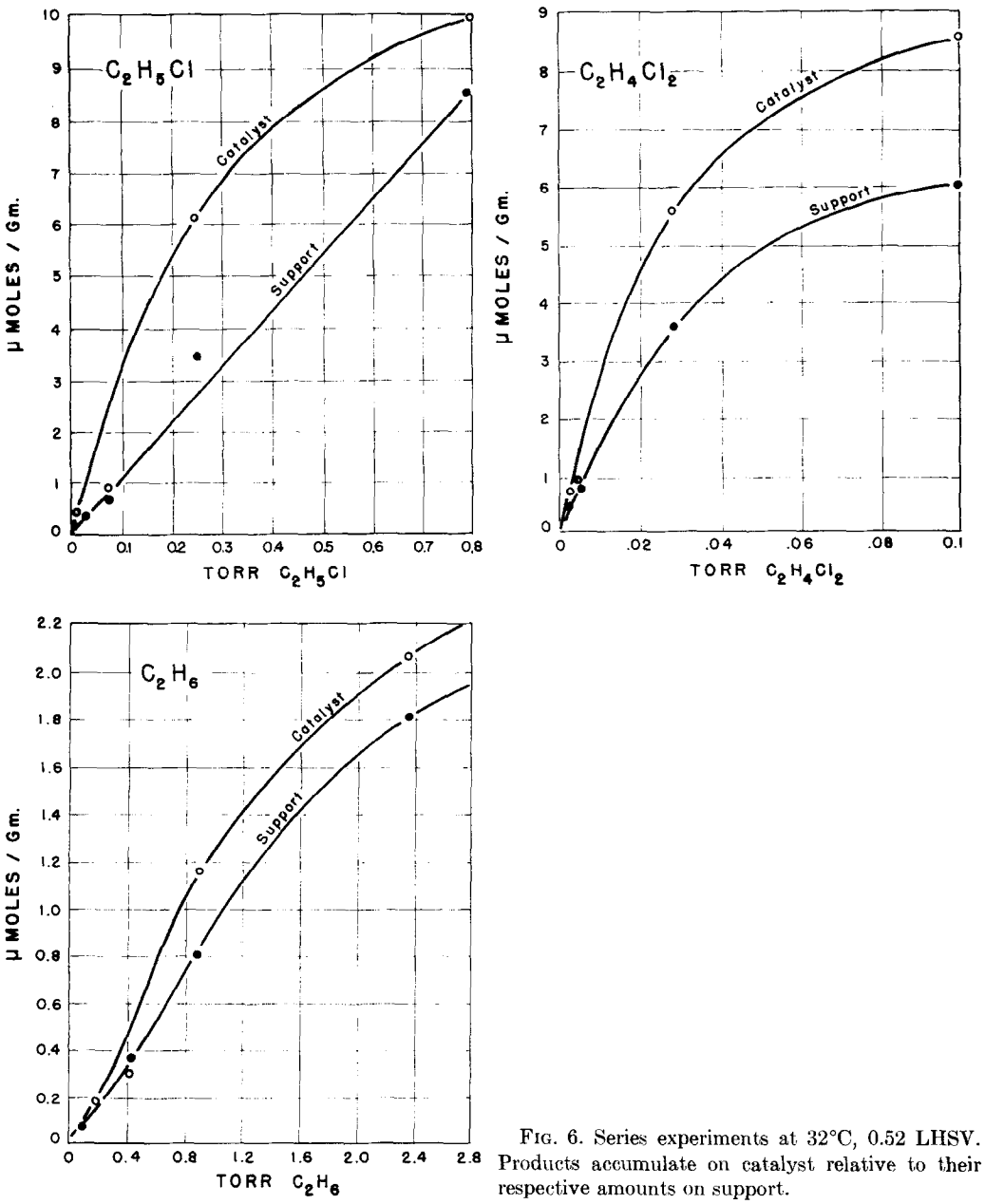

FIG. 6. Series experiments at 32°C, 0.52 LHSV. Products accumulate on catalyst relative to their respective amounts on support.

single pore. At low reaction rates C_i approaches C_0 and identical adsorption quantities of reacting and product species are measured on both the catalyst and support. At high reaction rates the observed depletion in the amounts of reacting species adsorbed on the catalyst compared with their relative amounts on support is due to (a) surface concentration gradients around the active Pt sites and (b) gas phase concentration gradient across the active pore length due to reaction.

The total amount N_T of reacting species measured on the catalyst is the sum of (a) the amount adsorbed in the pore at uniform concentration $C = C_i$ plus (b) the additional amount adsorbed on the active pore length due to the fact that in this region $C > C_i$.

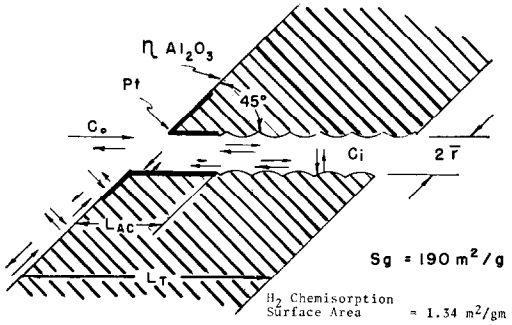

Wheeler's Working Rules

$$L_T = \frac{V_p}{S_x}\sqrt{2} = 460\,\mu$$

$$\bar{r} = 2\frac{V_g}{S_g} = 40.4\ \text{Å}$$

$$L_{AC} = \frac{V_{AC}}{S_x}\sqrt{2} = 37.6\,\mu$$

FIG. 7. Pore model for a peripherally deposited catalyst pellet.

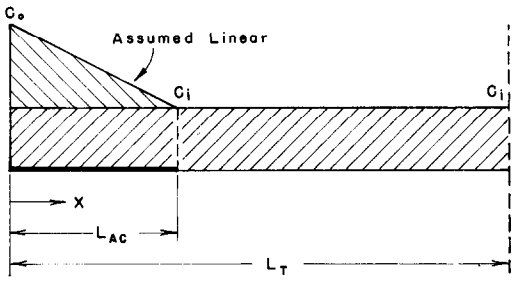

Co Measured Directly
Ci Calculated From Adsorption Isotherms
Boundary Conditions:

$X = 0 \quad C = C_o$

$X = L_{AC} \quad C = C_i, \ \frac{dc}{dx} = 0$

$X = L_T \quad C = C_i, \ \frac{dc}{dx} = 0$

$$D\frac{d^2C}{dx^2} = \frac{2kC^n}{\bar{r}}$$

FIG. 8. Peripherally deposited pore concentration gradients. The quantity of reacting species measured on the catalyst permits estimation of concentrations inside the pore.

C_i is calculated directly from the experimentally measured bulk gas concentration, total quantity adsorbed, and the support adsorption isotherm slope of Fig. 5, S.

$$C_i = \frac{(N_T/S) - (L_{Ac}/2L_T)C_0}{1 - (L_{Ac}/2L_T)} \qquad (3)$$

(using the assumption of a linear concentration gradient across the active metal).

The effectiveness factor for peripherally deposited catalyst can be defined as

$$\eta_{Ac} = \frac{\text{active length used for reaction at } C = C_0}{\text{total active length}}. \qquad (4)$$

This is shown on Fig. 9, and the effective-

$$\eta_{AC} = \frac{\text{Active Area Used For Reaction At } C = C_o}{\text{Total Active Area}}$$

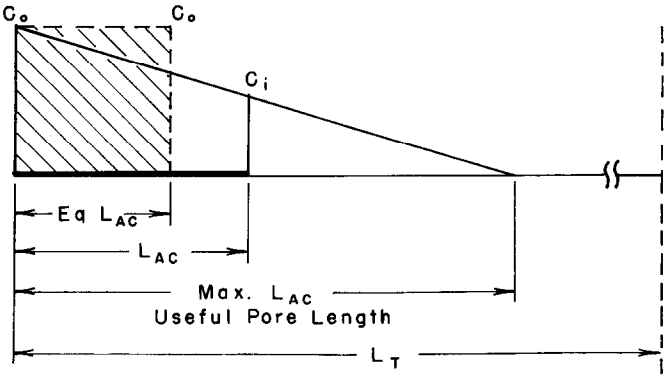

FIG. 9. Extrapolation of the gas concentration profile to the point where $C_i = 0$ gives an estimate of the useful pore depth for metal impregnation.

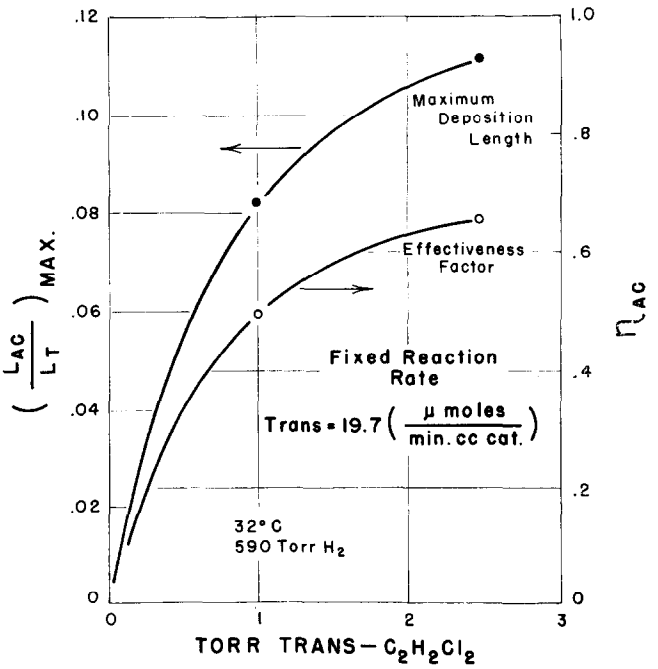

FIG. 10. Utilization of active metal. At fixed reaction rates, both η_{Ac} and max L_{Ac} increase with increasing reactant concentration.

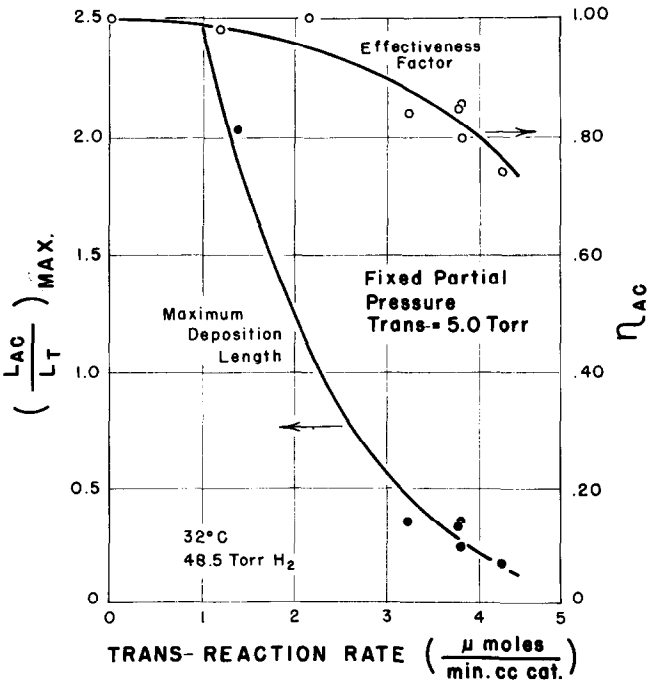

FIG. 11. Utilization of active metal. η_{Ac} and max L_{Ac} both increase with decreasing reaction rates at fixed reactant concentration.

ness factor for the active length of the pore where the metal is deposited, is

$$\eta_{Ac} = \frac{C_0 + C_i}{2C_0}. \quad (5)$$

If Pt were impregnated deeper into the pore more gas would react inside the pore for the same C_0. Extrapolation of the linear gas concentration profile on Fig. 9 to the point where $C_i = 0$, suggests that there is a maximum active Pt length, beyond which no reactant gas is available for reaction.

From the geometry of Fig. 9,

$$\max L_{Ac} = L_{Ac}\frac{C_0}{C_0 - C_i}, \quad (6)$$

and as $C_i \rightarrow C_0$, max $L_{Ac} \rightarrow \infty$.

Figure 10 is a plot of both the active metal effectiveness factor η_{Ac} and the fraction of the pore length that is useful for metal impregnation $(L_{Ac}/L_T)_{max}$ as a function of *trans*-$C_2H_2Cl_2$ partial pressure at fixed reaction rate of 19.2 μmoles/min cc cat. As would be expected, at fixed reaction rate, both effectiveness factor η_{Ac} and (max L_{Ac}) increase with increasing reactant concentration. Figure 11 shows the effect of *trans*-$C_2H_2Cl_2$ reaction rate on η_{Ac} and $(L_{Ac}/L_T)_{max}$ at fixed *trans*-partial pressure of 5.0 Torr. Both η_{Ac} and max L_{Ac} decrease with increasing reaction rates. Similar results were obtained for *cis*-$C_2H_2Cl_2$. More metal is utilized and greater pore depths can be used for metal deposition at low reaction rates and high reactant concentrations.

The solution to Eq. (1) for reaction order $n = 0$ in the active length L_{Ac} has also been given by Wheeler (*17*)

$$h = \left[2\left(1 - \frac{C_i}{C_0}\right)\right]^{1/2} = L_{Ac}\left(\frac{k_{Ac}}{D_{Ac}C_0\theta}\right)^{1/2} \quad (7)$$

where the experimentally measured reaction rate based on active metal length L_{Ac} equals the zero order rate constant k_{Ac}. The diffusion coefficient D_{Ac} for the peripherally impregnated pellet is then based on the active length L_{Ac} of the pore. This differs from the normal concept of diffusion coefficient based on the total length of a catalyst pore in a uniformly impregnated pellet. Table 4 lists diffusion coefficients across the active metal. The Knudsen diffusion coefficient D_K at the conditions of the experiments is larger than the values of D_{Ac}, possibly due to low permeability of the outer layers of the extruded catalyst pellet—the so-called "skin effects" (*19*). Scanning electron micro-

FIG. 12. SEM results on a fresh catalyst pellet. The fractured cross section of the catalyst pellet (right; ×1710) has a higher porosity than the surface exterior (left; ×1688), a skin effect from the extrusion process.

TABLE 4
SINGLE PORE DIFFUSIVITIES (cm^2/sec)
cis-$C_2H_2Cl_2$

P_0 (Torr)	Conv. (%)	$D_{Ac} = \frac{L_{Ac}^2 k_{Ac}}{\theta C_0 h^2}$
5.00	3.28	0.0025
5.17	5.75	0.0026
0.98	37.90	0.0023
2.47	39.20	0.0012

$D_k = 9700\bar{r}\left(\frac{T}{M}\right)^{1/2} = 0.0069$

$h = \left[2\left(1 - \frac{C_i}{C_0}\right)\right]^{1/2}$

$\epsilon = 1$ for $h < \sqrt{2}$

graphs for a reduced but unused catalyst pellet in Fig. 12 show that the fractured cross section has a higher porosity than the surface exterior. Since the diffusing reacting molecule has to pass through the external surface layer first, ideally the average pore radius $\bar{r}$ to be used in the calculation of D_{Ac} and D_K should be that of the pellet exterior and not that calculated from the experimentally determined ratio $2V_g/S_g$ (= 40.4 Å) for the whole pellet. A value of $\bar{r}$ lower than 40.4 Å will increase D_{Ac} and decrease D_K bringing the two values closer together.

CONCLUSIONS

In the system used for this work, the reaction of hydrogen with dichloroethylenes over 0.5% Pt peripherally deposited on $\frac{1}{16} \times \frac{1}{8}$ in. η-Al_2O_3 pellets, it was found that product HCl adsorption was high enough to displace significant quantities of dichloroethylenes. (This was not the case with hydrogen.) Even so, the depletion of reactants on the catalyst surface as a function of either conversion at fixed dichloroethylenes partial pressure or of partial pressure at fixed LHSV is significantly greater than can be accounted for by competitive adsorption of HCl produced in the reaction. The observed depletion of reactants on catalyst during reaction is believed to be a combined effect of surface and gas diffusion effects.

The technique of using a flow adsorption vessel tandem to the backmixed reactor and of flooding at steady state permits determination of adsorption isotherms on support at multicomponent partial pressures identical to those over the catalyst in the reactor. Such isotherms serve as the means for estimating the partial pressures inside a catalyst pore and behind a peripherally deposited active agent. With these data it then becomes possible to define an effectiveness factor η_{Ac} for a peripherally deposited catalyst and to predict the maximum useful depth that a catalytic agent should be impregnated into the pore. For rapid industrial reactions, such as reforming, pore diffusion limitations mitigate against impregnating noble metal uniformly along the length of a pore, since metal near the center of a pellet will not be utilized. On the other hand the useful pore length concept has the advantage of being an approach to "tailor" the depth of impregnation of a noble metal on a catalyst support to produce an economically optimum catalyst. The active metal effectiveness factor provides a measure of the efficiency of the metal utilization.

ACKNOWLEDGMENT

Acknowledgment is made to the donors of the Petroleum Research Fund, administered by the American Chemical Society, for their contribution to the support of this research. The authors are also indebted to Dr. William Manogue and E. I. duPont de Nemours & Co. for the transmission electron microscopic analyses and to Dr. Weldon K. Bell for his advice and suggestions.

REFERENCES

1. TAMARU, K., *in* "Advances in Catalysis" (D. D. Eley, H. Pines and P. B. Weisz, Eds.), Vol. 15, p. 65. Academic Press, New York, 1964.
2. VLASENKO, V. M., YOZEFOVICH, G. E., AND RUSOV, M. T., *Kinet. Katal.* **6**, 688 (1965).
3. CVETANOVIC, R. J., AND AMENOMIYA, Y., *in* "Advances in Catalysis" (D. D. Eley, H. Pines, and P. B. Weisz, Eds.), Vol. 17, p. 103. Academic Press, New York, 1967.
4. GAMBHIR, B. S., AND WEISS, A. H., *J. Catal.* **23**, 82 (1972).
5. WEISS, A. H., AND GAMBHIR, B. S., *Prepr. Pap. Int. Cong. Catal.*, Palm Beach, FL, Aug. 21–25, *1972*, Pap. No. 99.

6. ZELDOVICH, J. B., *Zh. Fiz. Khim.* **13,** 163 (1939).

7. ROITER, V. A., KORNEICHUK, G. P., LEPERSON, M. G., STUKANOWSKAIA, N. A., AND TOLCHINA, B. I., *Zh. Fiz. Khim.* **24,** 459 (1950).

8. HEGEDUS, L. L., AND PETERSON, E. E., *Ind. Eng. Chem. Fundam.* **11**(4), 579 (1972).

9. BALDER, J. R., AND PETERSON, E. E., *J. Catal.* **11,** 202 (1968).

10. BALDER, J. R., AND PETERSON, E. E., *Chem. Eng. Sci.* **23,** 1287 (1968).

11. WEISS, A. H., AND KRIEGER, K. A., *J. Catal.* **6,** 167 (1966).

12. GAMBHIR, B. S., PhD thesis, Worcester Polytechnic Inst., Worcester, MA, 1973.

13. ANDERSON, J. B., *Chem. Eng. Sci.* **18,** 147 (1963).

14. MEARS, D. E., *J. Catal.* **20,** 127 (1971).

15. BERCOVICH, S. E., AND JAIME, A. M., *J. Catal.* **22,** 64 (1971).

16. THIELE, E. W., *Ind. Eng. Chem.* **31,** 916 (1939).

17. WHEELER, A., *in* "Advances in Catalysis" (D. D. Eley, H. Pines, and P. B. Weisz, Eds.), Vol. 3, p. 249. Academic Press, New York, 1951.

18. WHEELER, A., *in* "Catalysis" (P. H. Emmett, Ed.), Vol. 2, p. 105. Reinhold, New York, 1955.

19. CADLE, P. J., AND SATTERFIELD, C. N., *Ind. Eng. Chem. Fundam.* **7,** 189 (1968).